ФИЗИКА ЭЛЕМЕНТАРНЫХ ЧАСТИЦ И АТОМНОГО ЯДРА
2016. Т. 47. ВЫП. 6

$\nu_\mu \to \nu_e$ OSCILLATIONS SEARCH IN THE OPERA EXPERIMENT

S. Zemskova[*] *on behalf of the OPERA Collaboration*

Joint Institute for Nuclear Research, Dubna

The tracking capabilities of the OPERA detector allow one to reconstruct τ leptons and electrons. It gives a possibility to observe $\nu_\mu \to \nu_\tau$ oscillations in the appearance mode and to study $\nu_\mu \to \nu_e$ oscillations in the ν_μ CNGS beam. Current results on $\nu_\mu \to \nu_e$ channel in the three-flavor mixing model are presented. The same data allow one to constrain the presence of additional sterile neutrino states. The analysis of the full 2008–2012 OPERA data set and work on its improvement are going on. Details of the achievements are presented.

PACS: 14.60.Lm; 14.60.St; 29.40.Rg; 29.40.Mc

INTRODUCTION

The main goal of the OPERA experiment [1] is an observation of $\nu_\mu \to \nu_\tau$ oscillations in the appearance mode through the detection of τ leptons in the ν_μ CNGS beam [2]. The OPERA detector is installed in Gran Sasso Underground Laboratory (LNGS), and the beam is produced at CERN SPS, 730 km away from the detector. The tracking capabilities of the nuclear emulsion used for the τ-lepton detection allow one to reconstruct electrons and to study $\nu_\mu \to \nu_e$ oscillations through the identification of electrons which are produced in ν_e charge current (CC) interactions. The parameters of the detector and the baseline make the experiment sensitive to the region of $\Delta m^2 > 0.01$ eV^2 (LSND [3] and MiniBooNE [4] allowed region) and capable to search for nonstandard oscillations.

1. OPERA DETECTOR, BEAM, DATA COLLECTION

The OPERA detector consists of two identical Super Modules (SM) and each of them has 31 scintillator planes (“Target Tracker” or TT) alternated with the Emulsion Cloud Chamber modules (ECC or “brick”) arranged in walls and a

[*]E-mail: zemskova@numail.jinr.ru

magnetic muon spectrometer. Detector contains 150,000 ECC and each of them consists of 57 emulsion films alternated by 56 1-mm lead plates. Each OPERA brick weighs 8.3 kg and has a removable doublet of emulsion films (Changeable Sheet or CS). CSs are on the downstream faces of the ECCs and they facilitate the neutrino interaction location.

Charged particles produced in the neutrino interactions left the TT signals which are used for the identification of the brick where neutrino interaction occurred. For each event the brick is extracted and the CS doublet is analyzed. If the tracks which were found in CS are converging or merged with TT data, the brick is developed and analyzed with the help of the modern high-speed automatic scanning microscopes which provide full information on neutrino interaction at the microscopic level.

The CNSG beam consists of ν_μ mainly. The contamination of $\overline{\nu}_\mu$, ν_e, and $\overline{\nu}_e$ is 2.1, 0.8, and 0.05% of ν_μ CC interactions, respectively.

The OPERA experiment collected data during 2008–2012 runs which correspond to $17.97 \cdot 10^{19}$ protons on target (p.o.t.), 18941 events were reconstructed. The $\nu_\mu \rightarrow \nu_e$ analysis is completed for the 2008–2009 data which correspond to $5.25 \cdot 10^{19}$ p.o.t. and to 5255 events recorded.

2. EMULSION SCANNING AND ν_e SEARCH

The bricks containing neutrino interactions are analyzed with the complex procedure described in detail in [5]. Here is a recalling of the main steps of the analysis.

TT predictions are used for the selection of the brick where interactions appeared and for the large area scan of the corresponding CS films. If the tracks found in CS match the TT signal, the emulsion films of the brick are developed and sent to the scanning labs. There with the help of the automatic microscopes the information from emulsion is read out and the scan-back procedure is applied; it means, each CS track candidate is followed upstream film by film to find the neutrino interaction vertex. Once the vertex is found, the scanning of a volume around the vertex is performed in order to reconstruct all the tracks connected to the vertex and to search for decay topologies.

The identification of an electron in ν_e CC interactions is based on the detection of the associated electromagnetic (EM) shower. Since the size of the standard scanning volume is too short to contain the EM shower, the systematic EM shower search in CS is applied. The procedure is sketched in Fig. 1.

If a shower is found, the corresponding shower track becomes an electron candidate. This track is inspected in the first two films downstream the vertex to check if the track is a single particle or an e^+e^- pair. This procedure allows one to reject EM shower initiated by the early conversion of γ from π^0 decay. Once

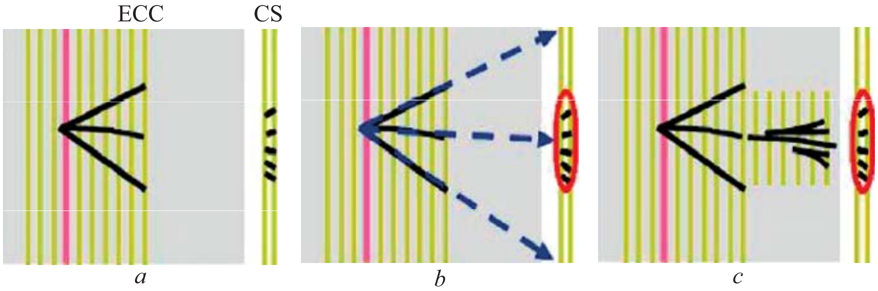

Fig. 1. Sketch of the procedure of a systematic search for ν_e candidates. After reconstruction of tracks in the standard volume (*a*), all tracks emerging from the interaction vertex are extrapolated to the CS (*b*). If three or more tracks with angular and spacial coordinates differing from a given track by $\Delta\theta < 150$ mrad and $\Delta x < 2$ mm are found in the CS, an additional volume along the full track length is scanned, leading to the possible detection of an EM shower (*c*) [6]

an electron track is confirmed at the interaction vertex, the event is classified as a ν_e candidate. The event energy is reconstructed from the TT data with the resolution:

$$\frac{\Delta E}{E} = 0.37 + \frac{0.74}{\sqrt{E}} \quad (E \text{ in GeV}). \tag{1}$$

In total, 2853 vertexes were located in the bricks during 2008–2009 runs and 505 of them were not classified as ν_μ CC interactions, out of them 19 ν_e candidates were found.

3. OSCILLATION ANALYSIS

3.1. Background $\nu_\mu \to \nu_e$ Appearance. There are several sources of background in the ν_e interaction identification: ν_e and $\overline{\nu}_e$ beam contamination, π_0 misidentification as an electron in neutrino interaction without a reconstructed muon, and ν_τ CC interactions with the decay of the τ to an electron.

In total, 19.8 ± 2.8 (syst.) background ν_e events are expected. This is in agreement with the 19 observed candidate ν_e events. Details of expected background are presented in Table 1, a more detailed description of background calculations is available in [6].

3.2. Three-Flavor Mixing Scenario. In the case of the standard three-flavor oscillation analysis the following parameters were used: $\sin^2(2\theta_{13}) = 0.098$, $\sin^2(2\theta_{23}) = 1$, $\Delta m^2_{32} = \Delta m^2_{31} = 2.32 \cdot 10^{-3}$ eV^2, assuming $\delta_{\rm CP} = 0$ and neglecting matter effects. In the whole energy range, 1.4 oscillated ν_e CC events were expected to be detected. The simulated and reconstructed energy distributions are presented in Fig. 2. The energy cut of 20 GeV was applied to improve

Table 1. **Expected and observed number of events for the different energy cuts [6]**

Background	Energy cut, GeV		
	20	30	No cut
BG common to both analyses			
BG from π^0	0.2	0.2	0.2
BG from $\tau \to e$	0.2	0.3	0.3
ν_e beam contamination	4.2	7.7	19.4
Total expected BG in the 3-flavor oscillation analysis	4.6	8.2	19.8
BG to nonstandard oscillation analysis only			
ν_e via 3-flavor oscillation	1.0	1.3	1.4
Total expected BG in the nonstandard oscillation analysis	5.6	9.4	21.3
Data	4	6	19

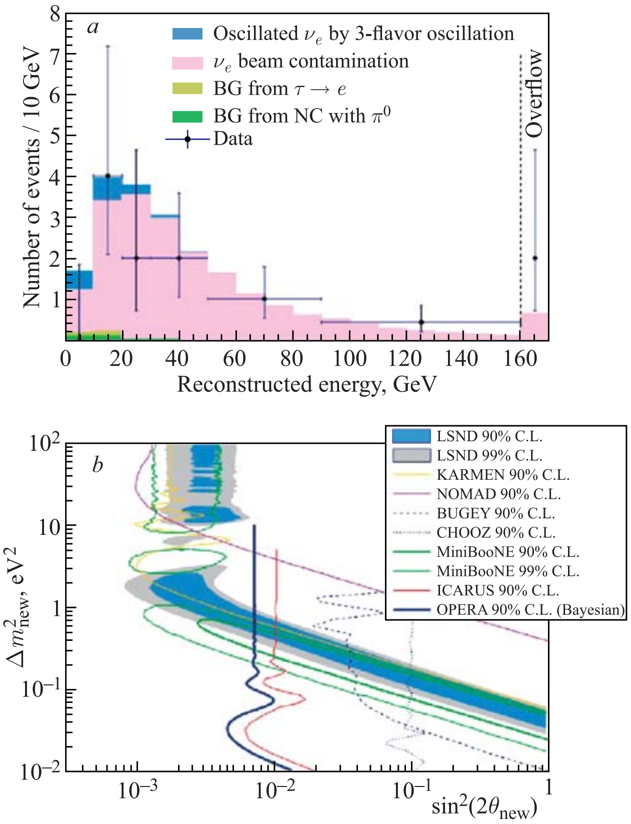

Fig. 2. *a*) Distribution of the reconstructed energy of the ν_e events and the expected spectrum from the different sources in a stack histogram, normalized to the number of p.o.t. analyzed. *b*) The exclusion plot in the plane of parameters of the nonstandard $\nu_\mu \to \nu_e$ oscillation, in the analysis using the Bayesian method [6]

Table 2. **90% C.L. upper limits and sensitivities on $\sin^2(2\theta_{\rm new})$, for different energy cuts, according to the F&C and Bayesian methods [6]**

Energy cut, GeV	Upper limit $\times 10^{-3}$		Sensitivity $\times 10^{-3}$	
	F&C	Bayes.	F&C	Bayes.
20	8.5	10.4	14.2	14.2
30	5.0	7.2	9.7	10.4
No cut	8.6	9.5	10.8	11.0

the signal to background ratio, increasing the sensitivity to θ_{13}. Details are given in Table 2. The number of observed events is compatible with the nonoscillation hypothesis and gives an upper limit for $\sin^2(2\theta_{13})$ of 0.44 with 90% C.L.

3.3. Nonstandard Oscillations. The OPERA data were used to search for the nonstandard oscillations indicated by LSND and MiniBooNE experiments. The conventional approach of expressing the $\nu_\mu \to \nu_e$ oscillation probability in the one mass scale dominance approximation was used:

$$P_{\nu_\mu \to \nu_e} = \sin^2(2\theta_{\rm new}) \sin^2(1.27 \Delta m^2{}_{\rm new} L({\rm km})/E({\rm GeV})). \qquad (2)$$

Note however that this approach does not allow a direct comparison between experiments working in different L/E regimes. Since the energy spectrum of the oscillated ν_e with $\Delta m^2_{\rm new} > 0.1$ eV^2 follows the spectrum of the ν_μ, which is almost vanishing above 40 GeV (Fig. 2), a cut on the reconstructed energy is introduced. The optimal cut on the reconstructed energy in terms of sensitivity is 30 GeV.

The number of observed events and expected backgrounds are represented in Table 1. Since the observed number of events is smaller than the expected background, both Feldman and Cousins (F&C) confidence interval [7] and the Bayesian bound, setting a prior to zero in the unphysical region and to a constant in the physical region [8], are provided (see Table 2).

Given the underfluctuation of the data, the curve with the Bayesian upper limit was chosen for the exclusion plot shown in Fig. 2. The results of other experiments, working in different L/E regimes, are also shown.

4. ANALYSIS IMPROVEMENT

4.1. The Increase of the Analyzed Data Sample and Location Efficiency Improvement. The most important directions of $\nu_\mu \to \nu_e$ analysis are the increase of statistics and the progress in location efficiency which will contribute in the reduction of the effect of the possible statistical underfluctuation of the background.

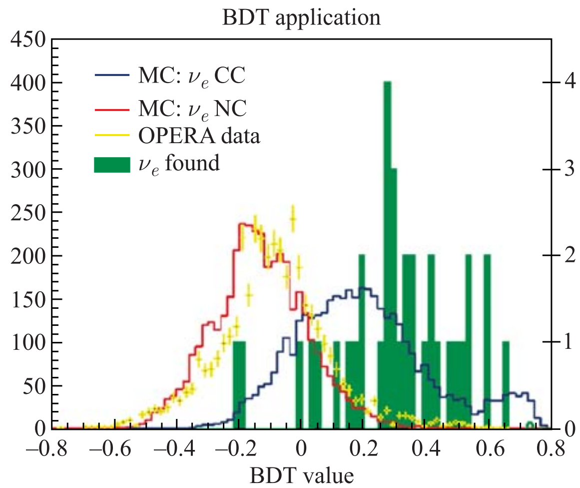

Fig. 3. Result of ν_μ NC and ν_e CC Monte Carlo events separation with a BDT algorithm and application to the OPERA data

The increase of statistics by a factor of 3.4 comparatively to 2008–2009 number of ν_e candidates is expected with the completion of the analysis of the collected data. So far, 52 ν_e candidates have been found.

The ν_e candidate search is based on the search for EM shower in CS doublets. This algorithm is quite efficient for the interactions which are located in the upstream part of the brick. If the interaction vertex is too close to the CS doublet, the EM shower has no enough space on its path for the development and it does not hint CS with three or more tracks as was shown in Fig. 1. An additional algorithm based on the TT data analysis was developed for the selection of the data fraction rich with the ν_e candidates. The separation of ν_μ NC and ν_e CC with a Boosted Decision Tree (BDT) algorithm [9] does not depend on the interaction vertex position in the brick and it is optimized for the oscillated ν_e energy region. The algorithm can be applied for a systematic ν_e search among the events with the black CS as well. The results of the algorithm training and the application to the OPERA data is shown in Fig. 3. The ν_e location efficiency is expected to be increased with usage of this algorithm.

4.2. Energy Reconstruction Improvement. There are other important improvements related to the ν_e energy reconstruction. The OPERA ED have rather limited resolution in the EM energy measurement due to:

• the sampling of the OPERA TT and the structure of TT planes: the energy deposit is visible every 10 radiation lengths only, the reconstruction of the

3-dimensional TT hits is impossible and the parts of the signal can flow from one photomultiplier channel to the neighboring channels;

• the saturation of the OPERA analog to digital converters (ADC): the saturation of the ADC gives a smaller signal amplitude in case of ~100 or more particles passing through the TT strip;

• the nonlinear dependence of resistive plate chamber (RPC) signal on the number of particles passing through them.

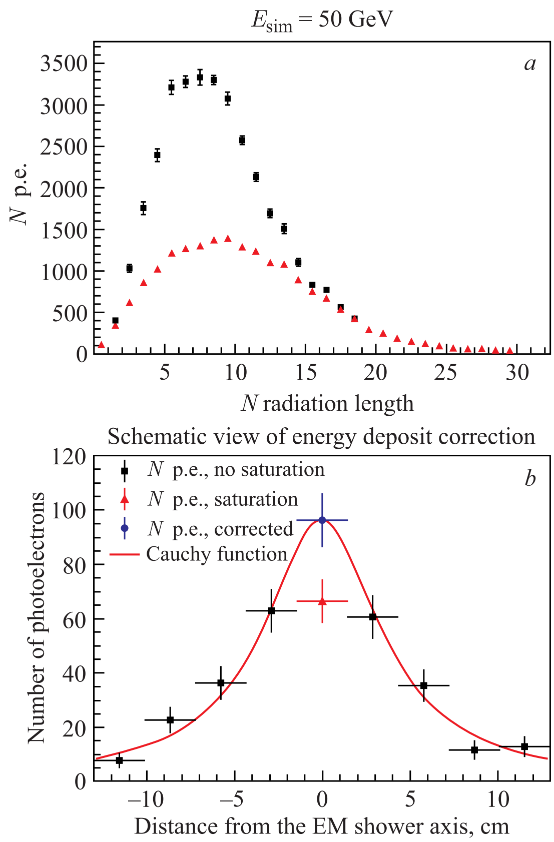

Fig. 4 (color online). *a*) The longitudinal EM shower profiles in the OPERA TT for an initial simulated electron energy of 50 GeV: the ADC saturation is not taken into account (in black, squares) and the ADC saturation is taken into account (in red, triangles). *b*) Shematic view of energy deposit correction: the signal of ADC without saturation (in black, squares), the signal of the ADC with the saturation (in red, triangles), recovered signal of the ADC with the saturation (in blue, circles) and a fit of the ADC signals without saturations used for the profile correction (red curve)

On the other hand, well-known transverse and longitudinal EM shower profiles can be used for the EM shower energy reconstruction [10, 11]. Since the vertex position and the direction of the electron which initiate the EM shower are known from the ECC data with the high precision, ECC data and ED data combination can be used to bypass above the limitations and to improve the energy resolution. The simulation of the electrons in OPERA detector shows that the saturation takes place for events with the initial electron energy higher than ~ 10 GeV and distort both longitudinal and transverse EM shower profiles, Fig. 4, *a*. As is shown in Fig. 4, *b*, the correction of the signal in the saturated channels is performed with help of the information from the neighboring channels using a fit of the transverse EM shower profile. The corrected energy deposit of the ν_e events and the longitudinal EM shower profile are shown in Fig. 5 in blue (curve *1* and circles). Figure 6 demonstrates the reconstructed energy of ν_e after the corrections applied and the comparison with the cases when the OPERA data without corrections is used and with the ideal case when there are no saturations in the OPERA detector.

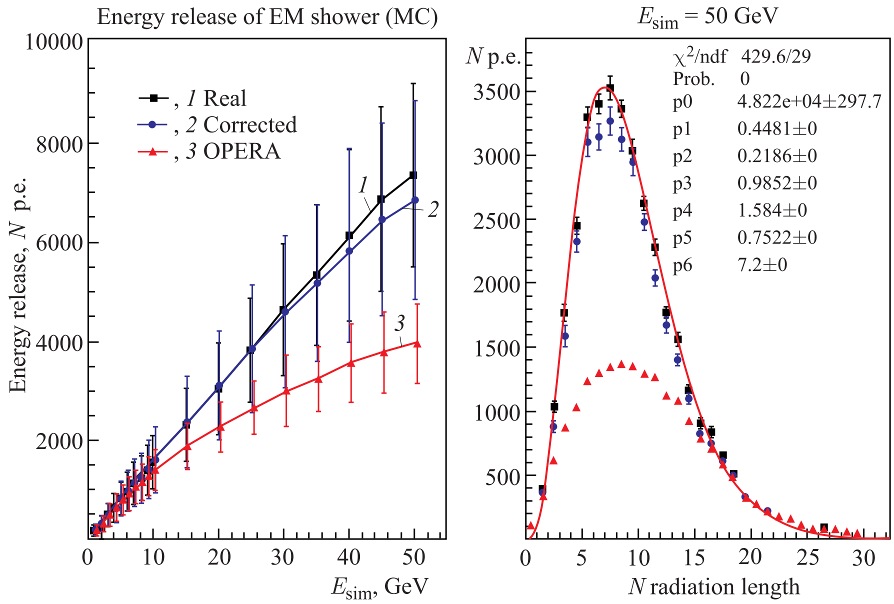

Fig. 5 (color online). Comparison of the OPERA detector response: no ADC signal saturation (in black, *1* and squares), with ADC signal saturation (in red, *3* and triangles); corrected response (in blue, *2* and circles). *a*) Calibration curve of the simulated electrons (the error bars are the standard deviation values). *b*) The longitudinal profile of the shower for 50-GeV electrons

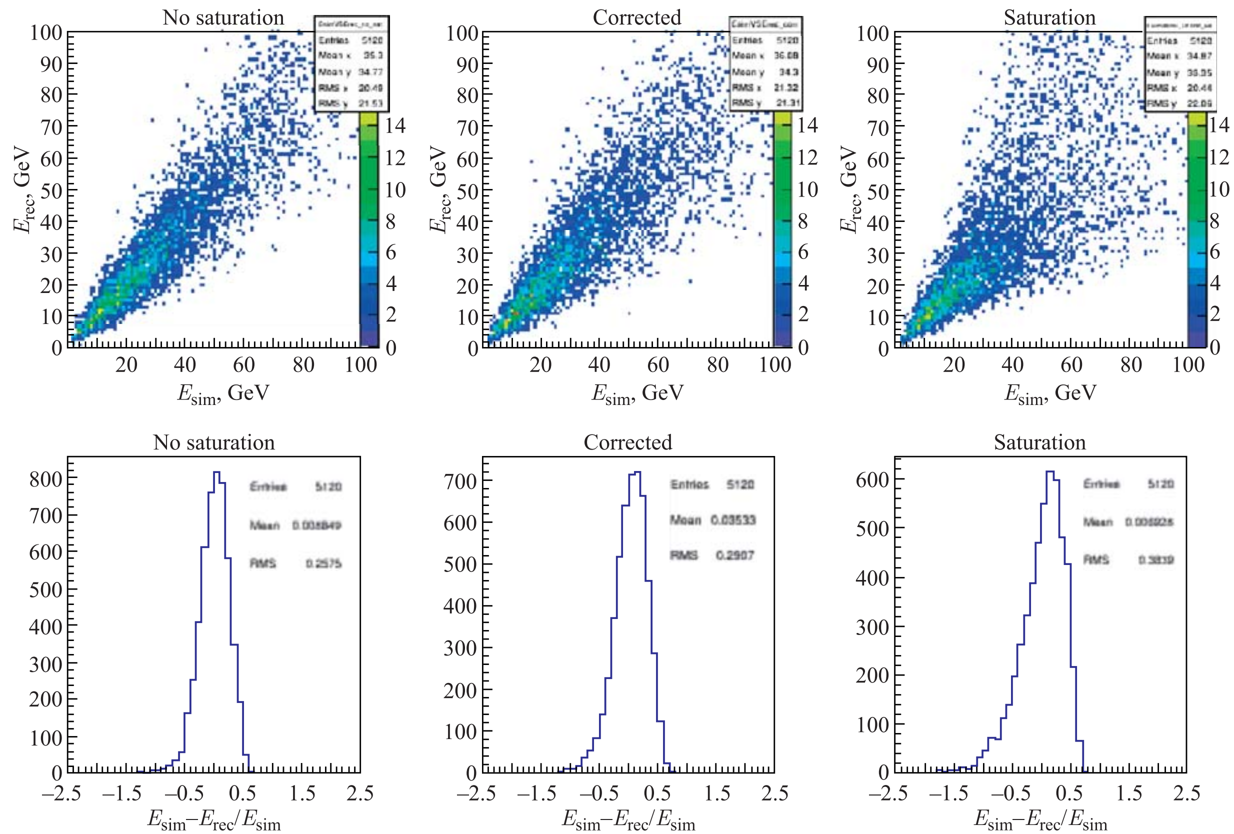

Fig. 6. Reconstructed energy ($E_{\rm rec}$) of ν_e events versus simulated energy ($E_{\rm sim}$) at the top and ($E_{\rm sim} - E_{\rm rec}/E_{\rm sim}$) at the bottom for 3 cases: without ADC saturation (left plot), corrected (central plot), and with ADC saturation (right plot)

CONCLUSIONS

During the runs of 2008–2012, the OPERA experiment has registered 18941 neutrino interactions in the target, corresponding to $17.97 \cdot 10^{19}$ p.o.t. The observed number of ν_e interactions in the data sample collected in the 2008–2009 runs ($5.25 \cdot 10^{19}$ p.o.t.) is 19 and it is compatible with the nonoscillation hypothesis. The current result on the search for the three-flavor neutrino oscillation yields a limit for the mixing angle $\sin^2(2\theta_{13}) < 0.44$ (90% C.L.). The OPERA results also limit the parameter space available for a nonstandard ν_e appearance. It further constrains the still allowed region around $\Delta m^2{}_{\rm new} > 5 \cdot 10^{-2}$ eV^2. For large Δm^2 values, the 90% C.L. upper limit on $\sin^2(2\theta_{\rm new})$ reaches $7.2 \cdot 10^{-3}$. The result is still affected by the statistical underfluctuation. With increase of statistics and the improvement of the energy resolution, the OPERA experiment is expected to reach the parameter region comparable with its sensitivity below $\sin^2(2\theta_{\rm new}) = 5 \cdot 10^{-3}$.

REFERENCES

1. *Guler M. et al. (OPERA Collab.).* An Appearance Experiment to Search for $\nu_\mu \leftrightarrow \nu_\tau$ Oscillations in the CNGS Beam: Experimental Proposal. CERN-SPSC-2000-028. 2000.
2. CNGS Project. http://proj-cngs.web.cern.ch/proj-cngs/.
3. *Aguilar-Arevalo A. et al. (LSND Collab.).* Evidence for Neutrino Oscillations from the Observation of $\bar{\nu_e}$ Appearance in a $\bar{\nu_\mu}$ Beam // Phys. Rev. D. 2001. V. 64. P. 112007.
4. *Aguilar-Arevalo A. et al. (MiniBooNE Collab.).* A Combined $\nu_\mu \to \nu_e$ & $\bar{\nu_\mu} \to \bar{\nu_e}$ Oscillation Analysis of the MiniBooNE Excesses. arXiv:1207.4809. 2012. 5 p.
5. *Agafonova N. et al. (OPERA Collab.).* Search for $\nu_\mu \to \nu_\tau$ Oscillations with the OPERA Experiment in the CNGS Beam // New J. Phys. 2012. V. 14. P. 033017.
6. *Agafonova N. et al. (OPERA Collab.).* Search for $\nu_\mu \to \nu_e$ Oscillations with the OPERA Experiment in the CNGS Beam // JHEP. 2013. V. 07, No. 04. 16 p.
7. *Feldman G. J., Cousins R. D.* Unified Approach to the Classical Statistical Analysis of Small Signals // Phys. Rev. D. 1998. V. 57. P. 3873.
8. *Gowan G.* Statistical Data Analysis. Oxford: Clarendon Press, 1998. 212 p.
9. *Hastie T., Tibshirani R., Friedman J.* The Elements of Statistical Learning: Data Mining, Interference, and Prediction. Second Ed. Springer, 2009. 758 p.
10. *Longo E., Sestili L.* Monte Carlo Calculation of Photon-Initiated Electromagnetic Showers in Lead Glass // Nucl. Instr. Meth. 1975. V. 128. P. 283–307.
11. *Grindhammer G., Peters S.* The Parameterized Simulation of Electromagnetic Showers in Homogeneous and Sampling Calorimeters. arXiv:hep-ex/0001020. 2000. 42 p.